

# INVERSE BOUNDARY VALUE PROBLEM FOR THE HELMHOLTZ EQUATION: QUANTITATIVE CONDITIONAL LIPSCHITZ STABILITY ESTIMATES

ELENA BERETTA\*, MAARTEN V. DE HOOP†, FLORIAN FAUCHER‡, AND OTMAR SCHERZER§

**Abstract.** We study the inverse boundary value problem for the Helmholtz equation using the Dirichlet-to-Neumann map at selected frequencies as the data. A conditional Lipschitz stability estimate for the inverse problem holds in the case of wavespeeds that are a linear combination of piecewise constant functions (following a domain partition) and gives a framework in which the scheme converges. The stability constant grows exponentially as the number of subdomains in the domain partition increases. We establish an order optimal upper bound for the stability constant. We eventually realize computational experiments to demonstrate the stability constant evolution for three dimensional wavespeed reconstruction.

**1. Introduction.** In this paper we study the inverse boundary value problem for the Helmholtz equation using the Dirichlet-to-Neumann map at selected frequencies as the data. This inverse problem arises, for example, in reflection seismology and inverse obstacle scattering problems for electromagnetic waves [3, 21, 4]. We consider wavespeeds containing discontinuities.

Uniqueness of the mentioned inverse boundary value problem was established by Sylvester & Uhlmann [20] assuming that the wavespeed is a bounded measurable function. This inverse problem has been extensively studied from an optimization point of view. We mention, in particular, the work of [5].

It is well known that the logarithmic character of stability of the inverse boundary value problem for the Helmholtz equation [1, 18] cannot be avoided, see also [13, 14]. In fact, in [16] Mandache proved that despite of regularity a priori assumptions of any order on the unknown wavespeed, logarithmic stability is the best possible. However, conditional Lipschitz stability estimates can be obtained: accounting for discontinuities, such an estimate holds if the unknown wavespeed is a finite linear combination of piecewise constant functions with an underlying known domain partitioning [6]. It was obtained following an approach introduced by Alessandrini and Vessella [2] and further developed by Beretta and Francini [7] for Electrical Impedance Tomography (EIT) based on the use of singular solutions. If, on one hand, this method allows to use partial data, on the other hand it does not allow to find an optimal bound of the stability constant. Here, we revisit the Lipschitz stability estimate for the full Dirichlet-to-Neumann map using complex geometrical optics (CGO) solutions which give rise to a sharp upper bound of the Lipschitz constant in terms of the number of subdomains in the domain partitioning. We develop the estimate in  $L^2(\Omega)$ .

Unfortunately, the use of CGO's solutions leads naturally to a dependence of the stability constant on frequency of exponential type. This is clearly far from being optimal as it is also pointed out in the paper of Nagayasu, Uhlmann and Wang [17]. There the authors prove a stability estimate, in terms of Cauchy data instead of the Dirichlet-to-Neumann map using CGO solutions. They derive a stability estimate consisting of two parts: a Lipschitz stability estimate and a Logarithmic stability estimate. When the frequency increases the logarithmic part decreases while the Lipschitz part becomes dominant but with a stability constant which blows up exponentially in frequency.

We can exploit the quantitative stability estimate, via a Fourier transform, in the corresponding time-domain inverse boundary value problem with bounded frequency data. Datchev and De Hoop [9] showed how to choose classes of non-smooth coefficient functions, one of which is consistent with the class considered here, so that optimization formulations of inverse wave problems satisfy the prerequisites for application of steepest descent and Newton-type iterative reconstruction methods. The proof is based on resolvent estimates for the Helmholtz equation. Thus, one can allow

\*Dipartimento di Matematica “Brioschi”, Politecnico di Milano, Italy ([elena.beretta@polimi.it](mailto:elena.beretta@polimi.it)).

†Department of Computational and Applied Mathematics and Department of Earth Science, Rice University, 6100 Main Street, Houston TX 77005, USA ([mdehoop@rice.edu](mailto:mdehoop@rice.edu)).

‡INRIA Bordeaux Sud-Ouest Research Center, Team Project Magique-3D, France ([florian.faucher@inria.fr](mailto:florian.faucher@inria.fr)).

§Computational Science Center, University of Vienna, Oskar-Morgenstern Platz 1, A-1090 Vienna, Austria ([otmar.scherzer@univie.ac.at](mailto:otmar.scherzer@univie.ac.at)).

approximate localization of the data in selected time windows, with size inversely proportional to the maximum allowed frequency. This is of importance to applications in the context of reducing the complexity of field data. We note that no information is lost by cutting out a (short) time window, since the boundary source functions (and wave solutions), being compactly supported in frequency, are analytic with respect to time. We cannot allow arbitrarily high frequencies in the data. This restriction is reflected, also, in the observation by Blazek, Stolk & Symes [8] that the adjoint equation, which appears in the mentioned iterative methods, does not admit solutions.

As a part of the analysis, we study the Fréchet differentiability of the direct problem and obtain the frequency and domain partitioning dependencies of the relevant constants away from the Dirichlet spectrum. Our results hold for finite fixed frequency data including frequencies arbitrarily close to zero while avoiding Dirichlet eigenfrequencies; in view of the estimates, inherently, there is a finest scale which can be reached. Finally we estimate the stability numerically and demonstrate the validity of the bounds, in particular in the context of reflection seismology.

## 2. Inverse boundary value problem with the Dirichlet-to-Neumann map as the data.

**2.1. Direct problem and forward operator.** We describe the direct problem and some properties of the data, that is, the Dirichlet-to-Neumann map. We will formulate the direct problem as a nonlinear operator mapping  $F_\omega$  from  $L^\infty(\Omega)$  to  $\mathcal{L}(H^{1/2}(\partial\Omega), H^{-1/2}(\partial\Omega))$  defined as

$$F_\omega(c^{-2}) = \Lambda_{\omega^2 c^{-2}},$$

where  $\Lambda_{\omega^2 c^{-2}}$  indicates the Dirichlet to Neumann operator. Indeed, at fixed frequency  $\omega^2$ , we consider the boundary value problem,

$$(2.1) \quad \begin{cases} (-\Delta - \omega^2 c^{-2}(x))u = 0, & \text{in } \Omega, \\ u = g & \text{on } \partial\Omega, \end{cases}$$

while  $\Lambda_{\omega^2 c^{-2}} : g \rightarrow \frac{\partial u}{\partial \nu}|_{\partial\Omega}$ , where  $\nu$  denotes the outward unit normal vector to  $\partial\Omega$ . In this section, we will state some known results concerning the well-posedness of problem (2.1) (see, for example, [11]) and regularity properties of the nonlinear map  $F_\omega$ . We will sketch the proofs of these results because we will need to keep track of the dependencies of the constants involved on frequency. We invoke

**ASSUMPTION 2.1.** *There exist two positive constants  $B_1, B_2$  such that*

$$(2.2) \quad B_1 \leq c^{-2} \leq B_2 \quad \text{in } \Omega.$$

In the sequel of Section 2  $C = C(a, b, c, \dots)$  indicates that  $C$  depends only on the parameters  $a, b, c, \dots$  and we will indicate different constants with the same letter  $C$ .

**PROPOSITION 2.2.** *Let  $\Omega$  be a bounded Lipschitz domain in  $\mathbb{R}^3$ ,  $f \in L^2(\Omega)$ ,  $g \in H^{1/2}(\partial\Omega)$  and  $c^{-2} \in L^\infty(\Omega)$  satisfying Assumption 2.1. Then, there exists a discrete set  $\Sigma_{c^{-2}} := \{\tilde{\lambda}_n \mid \tilde{\lambda}_n > 0, \forall n \in \mathbb{N}\}$  such that, for every  $\omega^2 \in \mathbb{C} \setminus \Sigma_{c^{-2}}$ , there exists a unique solution  $u \in H^1(\Omega)$  of*

$$(2.3) \quad \begin{cases} (-\Delta - \omega^2 c^{-2}(x))u = f & \text{in } \Omega, \\ u = g & \text{on } \partial\Omega. \end{cases}$$

Furthermore, there exists a positive constant  $C$  such that

$$(2.4) \quad \|u\|_{H^1(\Omega)} \leq C \left( 1 + \frac{\omega^2}{d(\omega^2, \Sigma_{c^{-2}})} \right) (\|g\|_{H^{1/2}(\partial\Omega)} + \|f\|_{L^2(\Omega)}),$$

where  $C = C(\Omega, B_2)$  and  $d(\omega^2, \Sigma_{c^{-2}})$  indicates the distance of  $\omega^2$  from  $\Sigma_{c^{-2}}$ .

*Proof.* We first prove the result for  $g = 0$ . Consider the linear operators  $-\Delta : H_0^1(\Omega) \rightarrow H^{-1}(\Omega)$  and the multiplication operator

$$(2.5) \quad \begin{aligned} M_{c^{-2}} : L^2(\Omega) &\rightarrow L^2(\Omega), \\ u &\rightarrow c^{-2}u \end{aligned}$$

respectively. We can now consider the operator  $K = \Delta^{-1}M_{c^{-2}} : H_0^1(\Omega) \rightarrow H_0^1(\Omega)$ . The equation

$$(-\Delta - \omega^2 c^{-2}(x))u = f.$$

for  $u \in H_0^1(\Omega)$  is equivalent to

$$(2.6) \quad (I - \omega^2 K)u = \Delta^{-1}f$$

Note that  $K : H_0^1(\Omega) \rightarrow H_0^1(\Omega)$  is compact by Rellich–Kondrachov compactness theorem. Furthermore, by Assumption 2.1 and the properties of  $\Delta^{-1}$  it follows that  $K$  is self-adjoint and positive. Hence,  $K$  has a discrete set of positive eigenvalues  $\{\alpha_n\}_{n \in \mathbb{N}}$  such that  $\alpha_n \rightarrow 0$  as  $n \rightarrow \infty$ . Let  $\tilde{\lambda}_n := \frac{1}{\alpha_n}$ ,  $n \in \mathbb{N}$  and define  $\Sigma_{c^{-2}} := \{\tilde{\lambda}_n : n \in \mathbb{N}\}$  and let  $\omega^2 \in \mathbb{C} \setminus \Sigma_{c^{-2}}$ , and show that it satisfies the assumptions of this proposition. Then, by the Fredholm alternative, there exists a unique solution  $u \in H_0^1(\Omega)$  of (2.6).

To prove estimate (2.4) we observe that

$$u = \sum_{n=1}^{\infty} \langle u, e_n \rangle e_n, \quad Ku = \sum_{n=1}^{\infty} \alpha_n \langle u, e_n \rangle e_n$$

where  $\{e_n\}_{n \in \mathbb{N}}$  is an orthonormal basis of  $L^2(\Omega)$ . Hence we can rewrite (2.6) in the form

$$\sum_{n=1}^{\infty} (1 - \omega^2 \alpha_n) \langle u, e_n \rangle e_n = \sum_{n=1}^{\infty} \langle h, e_n \rangle e_n \text{ where } h = \Delta^{-1}f$$

Hence,

$$\langle u, e_n \rangle = \frac{1}{1 - \frac{\omega^2}{\tilde{\lambda}_n}} \langle h, e_n \rangle, \quad \forall n \in \mathbb{N}$$

and

$$u = \sum_{n=1}^{\infty} \frac{1}{1 - \frac{\omega^2}{\tilde{\lambda}_n}} \langle h, e_n \rangle e_n$$

so that

$$(2.7) \quad \|u\|_{L^2(\Omega)} \leq \left(1 + \frac{\omega^2}{d(\omega^2, \Sigma_{c^{-2}})}\right) \|h\|_{L^2(\Omega)} \leq C \left(1 + \frac{\omega^2}{d(\omega^2, \Sigma_{c^{-2}})}\right) \|f\|_{L^2(\Omega)}$$

where  $C = C(\Omega, B_2)$ .

Now, by multiplying equation (2.3) with  $u$ , integrating by parts, using Schwartz' inequality, Assumptions (2.1) and (2.7) it follows in the case  $g = 0$ :

$$(2.8) \quad \|\nabla u\|_{L^2(\Omega)} \leq C \left(1 + \frac{\omega^2}{d(\omega^2, \Sigma_{c^{-2}})}\right) \|f\|_{L^2(\Omega)}$$

Hence, by (2.7) and (2.8) we finally get

$$\|u\|_{H^1(\Omega)} \leq C \left(1 + \frac{\omega^2}{d(\omega^2, \Sigma_{c^{-2}})}\right) \|f\|_{L^2(\Omega)}.$$

If  $g$  is not identically zero then we reduce the problem to the previous case by considering  $v = u - \tilde{g}$  where  $\tilde{g} \in H^1(\Omega)$  is such that  $\tilde{g} = g$  on  $\partial\Omega$  and  $\|\tilde{g}\|_{H^1(\Omega)} \leq \|g\|_{H^{1/2}(\partial\Omega)}$  and we derive easily the estimate

$$\|u\|_{H^1(\Omega)} \leq C \left( 1 + \frac{\omega^2}{d(\omega^2, \Sigma_{c^{-2}})} \right) (\|f\|_{L^2(\Omega)} + \|g\|_{H^{1/2}(\partial\Omega)})$$

which concludes the proof.  $\square$

The constants appearing in the estimate of Proposition 2.2 depends on  $c^{-2}$  and  $\Sigma_{c^{-2}}$  which are unknown. To our purposes it would be convenient to have constants depending only on a priori parameters  $B_1, B_2$  and other known parameters. Let us denote by  $\Sigma_0$  the spectrum of  $-\Delta$ . Then, we have the following

**PROPOSITION 2.3.** *Suppose that the assumptions of Proposition 2.2 are satisfied. Let  $\{\lambda_n\}_{n \in \mathbb{N}}$  denote the Dirichlet eigenvalues of  $-\Delta$ . Then, for any  $n \in \mathbb{N}$ ,*

$$(2.9) \quad \frac{\lambda_n}{B_2} \leq \tilde{\lambda}_n \leq \frac{\lambda_n}{B_1}.$$

If  $\omega^2$  is such that,

$$(2.10) \quad 0 < \omega^2 < \frac{\lambda_1}{B_2},$$

or, for some  $n \geq 1$ ,

$$(2.11) \quad \frac{\lambda_n}{B_1} < \omega^2 < \frac{\lambda_{n+1}}{B_2},$$

then there exists a unique solution  $u \in H^1(\Omega)$  of Problem 2.1 and the following estimate holds

$$\|u\|_{H^1(\Omega)} \leq C (\|g\|_{H^{1/2}(\partial\Omega)} + \|f\|_{L^2(\Omega)}),$$

where  $C = C(B_1, B_2, \omega^2, \Sigma_0)$ .

*Proof.* To derive estimate (2.9) we consider the Rayleigh quotient related to equation (2.1)

$$\frac{\int_{\Omega} |\nabla v|^2}{\int_{\Omega} c^{-2} v^2}.$$

By Assumption 2.1, for any non trivial  $v \in H_0^1(\Omega)$ ,

$$\frac{1}{B_2} \frac{\int_{\Omega} |\nabla v|^2}{\int_{\Omega} v^2} \leq \frac{\int_{\Omega} |\nabla v|^2}{\int_{\Omega} c^{-2} v^2} \leq \frac{1}{B_1} \frac{\int_{\Omega} |\nabla v|^2}{\int_{\Omega} v^2},$$

which, by the Courant-Rayleigh minimax principle, immediately gives

$$\frac{\lambda_n}{B_2} \leq \tilde{\lambda}_n \leq \frac{\lambda_n}{B_1}, \quad \forall n \in \mathbb{N}.$$

Hence, we have well-posedness of problem (2.1) if we select an  $\omega^2$  satisfying (2.10) or (2.11) and the claim follows.  $\square$

In the seismic application we have in mind we might know the spectrum of some reference wavespeed  $c_0^{-2}$ . The following local result holds

PROPOSITION 2.4. *Let  $\Omega$  and  $c_0^{-2}$  satisfy the assumptions of Proposition 2.2 and let  $\omega^2 \in \mathbb{C} \setminus \Sigma_{c_0^{-2}}$  where  $\Sigma_{c_0^{-2}}$  is the Dirichlet spectrum of equation (2.1) corresponding to  $c_0^{-2}$ . Then, there exists  $\delta = \delta(\Omega, \omega^2, B_2, \Sigma_{c_0^{-2}}) > 0$  such that, if*

$$\|c^{-2} - c_0^{-2}\|_{L^\infty(\Omega)} \leq \delta,$$

*then  $\omega^2 \in \mathbb{C} \setminus \Sigma_{c^{-2}}$  and the solution  $u$  of Problem 2.3 corresponding to  $c^{-2}$  satisfies*

$$\|u\|_{H^1(\Omega)} \leq C \left( 1 + \frac{\omega^2}{d(\omega^2, \Sigma_{c_0^{-2}})} \right) (\|f\|_{L^2(\Omega)} + \|g\|_{H^{1/2}(\partial\Omega)}),$$

$C = C(\Omega, B_2)$ .

*Proof.* Let  $\delta_c := c^{-2} - c_0^{-2}$  and consider  $u_0 \in H^1(\Omega)$  the unique solution of 2.3 for  $c_0^{-2}$  and consider the problem

$$(2.12) \quad \begin{cases} -\Delta v - \omega^2 c_0^{-2} v - \omega^2 \delta_c v = \omega^2 u_0 \delta_c & \text{in } \Omega, \\ v = 0, & \text{on } \partial\Omega. \end{cases}$$

Let now

$$L := -\Delta - \omega^2 c_0^{-2}$$

then, by assumption, it is invertible from  $H_0^1(\Omega)$  to  $L^2(\Omega)$  and we can rewrite problem (2.12) in the form

$$(2.13) \quad (I - K)v = h,$$

where  $K = \omega^2 L^{-1} M_{\delta_c}$  and  $M_{\delta_c}$  is the multiplication operator defined in (2.5) and  $h = L^{-1}(\omega^2 u_0 \delta_c)$ . Observe now that from (2.4)  $\|L^{-1}\| \leq C(1 + \frac{\omega^2}{d_0})$  with  $C = C(\Omega, B_2)$  and where  $d_0 = \text{dist}(\omega^2, \Sigma_{c_0^{-2}})$ . Hence, we derive

$$\|K\| \leq \omega^2 \|L^{-1}\| \|M_{\delta_c}\| \leq \omega^2 \|L^{-1}\| \delta \leq C \omega^2 (1 + \frac{\omega^2}{d_0}) \delta.$$

Hence, choosing  $\delta = \frac{1}{2}(C \omega^2 (1 + \frac{\omega^2}{d_0}))^{-1}$  the bounded operator  $K$  has norm smaller than one. Hence,  $I - K$  is invertible and there exists a unique solution  $v$  of (2.13) in  $H_0^1$  satisfying (2.4) with  $C = C(B_2, \omega^2, \Omega, d_0)$  and since  $u = u_0 + v$  the statement follows.  $\square$

On the basis of the previous results the direct operator,  $F_\omega$

$$\begin{aligned} F_\omega : L^\infty(\Omega) &\rightarrow \mathcal{L}(H^{1/2}(\partial\Omega), H^{-1/2}(\partial\Omega)), \\ c^{-2}(x) &\mapsto \Lambda_{\omega^2 c^{-2}}, \end{aligned}$$

is well defined for  $\omega^2 \in \mathbb{C} \setminus \Sigma_{c^{-2}}$ . We will examine its regularity properties in the following lemmas. We will show the Fréchet differentiability of the map  $F_\omega$ .

LEMMA 2.5 (Fréchet differentiability). *Let  $c^{-2} \in L^\infty(\Omega)$  satisfy Assumption (2.1). Assume that  $\omega^2 \in \mathbb{C} \setminus \Sigma_{c^{-2}}$ . Then, the direct operator  $F_\omega$  is Fréchet differentiable at  $c^{-2}$  and its Fréchet derivative  $DF_\omega(c^{-2})$  satisfies*

$$(2.14) \quad \|DF_\omega[c^{-2}]\|_{\mathcal{L}(L^\infty(\Omega), \mathcal{L}(H^{1/2}(\partial\Omega), H^{-1/2}(\partial\Omega)))} \leq C \omega^2 \left( 1 + \frac{\omega^2}{d(\omega^2, \Sigma_{c^{-2}})} \right)^2$$

where  $C = C(\Omega, B_2)$ .

*Proof.* Consider  $c^{-2} + \delta c^{-2}$ . Then, from Proposition 2.4, if  $\|\delta c^{-2}\|_{L^\infty}(\Omega)$  is small enough,  $\omega^2 \notin \Sigma_{c^{-2} + \delta c^{-2}}$ . An application of Alessandrini's identity then gives

$$(2.15) \quad \langle (\Lambda_{\omega^2(c^{-2} + \delta c^{-2})} - \Lambda_{\omega^2 c^{-2}})g, h \rangle = \omega^2 \int_{\Omega} \delta c^{-2} uv \, dx,$$

where where  $\langle \cdot, \cdot \rangle$  is the dual pairing with respect to  $H^{-1/2}(\partial\Omega)$  and  $H^{1/2}(\partial\Omega)$  and  $u$  and  $v$  solve the boundary value problems,

$$\begin{cases} (-\Delta - \omega^2(c^{-2} + \delta c^{-2}))u = 0, & x \in \Omega, \\ u = g, & x \in \partial\Omega, \end{cases}$$

and

$$\begin{cases} (-\Delta - \omega^2 c^{-2})v = 0, & x \in \Omega, \\ v = h, & x \in \partial\Omega, \end{cases}$$

respectively. We first show that the map  $F_\omega$  is Fréchet differentiable and that the Fréchet derivative is given by

$$(2.16) \quad \langle DF_\omega[c^{-2}](\delta c^{-2})g, h \rangle = \omega^2 \int_{\Omega} \delta c^{-2} \tilde{u}v \, dx,$$

where  $\tilde{u}$  solves the equation

$$\begin{cases} (-\Delta - \omega^2 c^{-2})\tilde{u} = 0, & x \in \Omega, \\ \tilde{u} = g, & x \in \partial\Omega. \end{cases}$$

In fact, by (2.15), we have that

$$(2.17) \quad \langle (\Lambda_{\omega^2(c^{-2} + \delta c^{-2})} - \Lambda_{\omega^2 c^{-2}})g, h \rangle - \omega^2 \int_{\Omega} \delta c^{-2} \tilde{u}v \, dx = \omega^2 \int_{\Omega} \delta c^{-2} (u - \tilde{u})v \, dx.$$

We note that  $u - \tilde{u}$  solves the equations

$$\begin{cases} (-\Delta - \omega^2 c^{-2})(u - \tilde{u}) = -\omega^2 \delta c^{-2} u, & x \in \Omega, \\ u - \tilde{u} = 0, & x \in \partial\Omega. \end{cases}$$

Using the fact that  $u - \tilde{u}$  and  $v$  are in  $H^1(\Omega)$  and that  $\delta c^{-2} \in L^\infty(\Omega)$  and applying Cauchy-Schwarz inequality, we get

$$(2.18) \quad \left| \omega^2 \int_{\Omega} \delta c^{-2} (u - \tilde{u})v \, dx \right| \leq \omega^2 \|\delta c^{-2}\|_{L^\infty} \|\|u - \tilde{u}\|_{L^2} \|v\|_{L^2} \right|.$$

Finally, using the stability estimates of Proposition 2.2 applied to  $u - \tilde{u}$  and to  $v$  and the stability estimates of Proposition 2.4 applied to  $u$  we derive

$$(2.19) \quad \left| \omega^2 \int_{\Omega} \delta c^{-2} (u - \tilde{u})v \, dx \right| \leq C\omega^4 \left( 1 + \frac{\omega^2}{d(\omega^2, \Sigma_{c^{-2}})} \right)^3 \|\delta c^{-2}\|_{L^\infty}^2 \|g\|_{H^{1/2}(\partial\Omega)} \|h\|_{H^{1/2}(\partial\Omega)}.$$

Hence

$$\begin{aligned} & \left| \langle (\Lambda_{\omega^2(c^{-2} + \delta c^{-2})} - \Lambda_{\omega^2 c^{-2}})g, h \rangle - \omega^2 \int_{\Omega} \delta c^{-2} \tilde{u}v \, dx \right| \\ & \leq C\omega^4 \left( 1 + \frac{\omega^2}{d(\omega^2, \Sigma_{c^{-2}})} \right)^3 \|\delta c^{-2}\|_{L^\infty}^2 \|g\|_{H^{1/2}(\partial\Omega)} \|h\|_{H^{1/2}(\partial\Omega)}, \end{aligned}$$

which proves differentiability.

Finally by

$$\langle DF_\omega[c^{-2}](\delta c^{-2})g, h \rangle = \omega^2 \int_\Omega \delta c^{-2} \tilde{u}v \, dx,$$

and we get

$$\begin{aligned} |\langle DF_\omega[c^{-2}](\delta c^{-2})g, h \rangle| &\leq \omega^2 \|\delta c^{-2}\|_{L^\infty(\Omega)} \|\tilde{u}\|_{L^2(\Omega)} \|v\|_{L^2(\Omega)} \\ &\leq \omega^2 \left(1 + \frac{\omega^2}{d(\omega^2, \Sigma_{c^{-2}})}\right)^2 \|\delta c^{-2}\|_{L^\infty(\Omega)} \|g\|_{H^{1/2}(\partial\Omega)} \|h\|_{H^{1/2}(\partial\Omega)}. \end{aligned}$$

from which (2.14) follows.  $\square$

**2.2. Conditional quantitative Lipschitz stability estimate.** Let  $B_2, r_0, r_1, A, L, N$  be positive with  $N \in \mathbb{N}, N \geq 2, r_0 < 1$ . In the sequel we will refer to these numbers as to the a priori data. To prove the results of this section we invoke the following common assumptions

ASSUMPTION 2.6.  $\Omega \subset \mathbb{R}^3$  is a bounded domain such that

$$|x| \leq Ar_1, \quad \forall x \in \Omega.$$

Moreover,

$\partial\Omega$  of Lipschitz class with constants  $r_1$  and  $L$ .

Let  $\mathcal{D}_N$  be a partition of  $\Omega$  given by

$$(2.20) \quad \mathcal{D}_N \triangleq \left\{ \{D_1, D_2, \dots, D_N\} \mid \bigcup_{j=1}^N \overline{D}_j = \Omega, (D_j \cap D_{j'})^\circ = \emptyset, j \neq j' \right\}$$

such that

$\{\partial D_j\}_{j=1}^N$  is of Lipschitz class with constants  $r_0$  and  $L$ .

ASSUMPTION 2.7. The function  $c^{-2} \in \mathcal{W}_N$ , that is, it satisfies

$$B_1 \leq c^{-2} \leq B_2, \quad \text{in } \Omega$$

and is of the form

$$c^{-2}(x) = \sum_{j=1}^N c_j \chi_{D_j}(x),$$

where  $c_j, j = 1, \dots, N$  are unknown numbers and  $\{D_1, \dots, D_N\} \in \mathcal{D}_N$ .

ASSUMPTION 2.8. Assume

$$0 < \omega^2 < \frac{\lambda_1}{B_2},$$

or, for some  $n \geq 1$ ,

$$\frac{\lambda_n}{B_1} < \omega^2 < \frac{\lambda_{n+1}}{B_2}.$$

Under the above assumptions we can state the following preliminary result

LEMMA 2.9. *Let  $\Omega$  and  $\mathcal{D}_N$  satisfy Assumption (2.6) and let  $c^{-2} \in \mathcal{W}_N$ . Then, for every  $s' \in (0, 1/2)$ , there exists a positive constant  $C$  with  $C = C(L, s')$  such that*

$$(2.21) \quad \|c^{-2}\|_{H^{s'}(\Omega)} \leq C(L, s') \frac{1}{r_0^{s'}} \|c^{-2}\|_{L^2(\Omega)}.$$

*Proof.* The proof is based on the extension of a result of Magnanini and Papi in [15] to the three dimensional setting. In fact, following the argument in [15], one has that

$$(2.22) \quad \|\chi_{D_j}\|_{H^{s'}(\Omega)}^2 \leq \frac{16\pi}{(1-2s')(2s')^{1+2s'}} |D_j|^{1-2s'} |\partial D_j|^{2s'}.$$

We now use the fact that  $\{D_j\}_{j=1}^N$  is a partition of disjoint sets of  $\Omega$  to show the following inequality

$$(2.23) \quad \|c^{-2}\|_{H^{s'}(\Omega)}^2 \leq 2 \sum_{j=1}^N c_j^2 \|\chi_{D_j}\|_{H^{s'}(\Omega)}^2$$

In fact, in order to prove (2.23) recall that

$$\|c^{-2}\|_{H^{s'}(\Omega)}^2 = \int_{\Omega} \int_{\Omega} \frac{|\sum_{j=1}^N c_j (\chi_{D_j}(x) - \chi_{D_j}(y))|^2}{|x-y|^{3+2s'}} dx dy$$

and observe that, since the  $\{D_j\}_{j=1}^N$  is a partition of disjoint sets of  $\Omega$ , we get

$$|\sum_{j=1}^N c_j (\chi_{D_j}(x) - \chi_{D_j}(y))|^2 = \sum_{j=1}^N c_j^2 (\chi_{D_j}(x) - \chi_{D_j}(y))^2 - \sum_{i \neq j} c_i c_j \chi_{D_i}(x) \chi_{D_j}(y)$$

Again, by the fact that the  $\{D_j\}_{j=1}^N$  are disjoint sets, we have

$$\begin{aligned} \sum_{i \neq j} |c_i c_j| \chi_{D_i}(x) \chi_{D_j}(y) &\leq \sum_{i \neq j} \frac{c_i^2 + c_j^2}{2} \chi_{D_i}(x) \chi_{D_j}(y) \\ &= \sum_{i \neq j} \frac{c_i^2}{2} (\chi_{D_i}(x) - \chi_{D_i}(y))^2 \chi_{D_i}(x) \chi_{D_j}(y) + \sum_{i \neq j} \frac{c_j^2}{2} (\chi_{D_j}(x) - \chi_{D_j}(y))^2 \chi_{D_i}(x) \chi_{D_j}(y) \\ &\leq \sum_{i \neq j} \frac{c_i^2}{2} (\chi_{D_i}(x) - \chi_{D_i}(y))^2 \chi_{D_j}(y) + \sum_{i \neq j} \frac{c_j^2}{2} (\chi_{D_j}(x) - \chi_{D_j}(y))^2 \chi_{D_i}(x) \\ &\leq \sum_{i=1}^N \frac{c_i^2}{2} (\chi_{D_i}(x) - \chi_{D_i}(y))^2 \sum_{j=1}^N \chi_{D_j}(y) + \sum_{j=1}^N \frac{c_j^2}{2} (\chi_{D_j}(x) - \chi_{D_j}(y))^2 \sum_{i=1}^N \chi_{D_i}(y) \\ &\leq \sum_{i=1}^N \frac{c_i^2}{2} (\chi_{D_i}(x) - \chi_{D_i}(y))^2 + \sum_{j=1}^N \frac{c_j^2}{2} (\chi_{D_j}(x) - \chi_{D_j}(y))^2 \\ &= \sum_{i=1}^N c_i^2 (\chi_{D_i}(x) - \chi_{D_i}(y))^2 \end{aligned}$$

where we have used the fact that  $\sum_{i=1}^N \chi_{D_i} \leq 1$ . So, we have derived that

$$|\sum_{j=1}^N c_j (\chi_{D_j}(x) - \chi_{D_j}(y))|^2 \leq 2 \sum_{j=1}^N c_j^2 (\chi_{D_j}(x) - \chi_{D_j}(y))^2$$

from which it follows that

$$\begin{aligned}
\|c^{-2}\|_{H^{s'}(\Omega)}^2 &= \int_{\Omega} \int_{\Omega} \frac{|\sum_{j=1}^N c_j (\chi_{D_j}(x) - \chi_{D_j}(y))|^2}{|x-y|^{3+2s'}} dx dy \\
&\leq 2 \int_{\Omega} \int_{\Omega} \frac{\sum_{j=1}^N c_j^2 (\chi_{D_j}(x) - \chi_{D_j}(y))^2}{|x-y|^{3+2s'}} dx dy \\
&\leq 2 \sum_{j=1}^N c_j^2 \int_{\Omega} \int_{\Omega} \frac{(\chi_{D_j}(x) - \chi_{D_j}(y))^2}{|x-y|^{3+2s'}} dx dy = 2 \sum_{j=1}^N c_j^2 \|\chi_{D_j}\|_{H^{s'}(\Omega)}^2
\end{aligned}$$

which proves (2.23). so that finally from (2.23), (2.22) and from Assumption (2.6) we get

$$\|c^{-2}\|_{H^{s'}(\Omega)}^2 \leq 2 \sum_{j=1}^N c_j^2 \|\chi_{D_j}\|_{H^{s'}(\Omega)}^2 \leq C(s') \sum_{j=1}^N c_j^2 |D_j| \left( \frac{|\partial D_j|}{|D_j|} \right)^{2s'} \leq \frac{C(L, s')}{r_0^{2s'}} \|c^{-2}\|_{L^2(\Omega)}^2.$$

□

We are now ready to state and prove our main stability result

**PROPOSITION 2.10.** *Assume (2.6) and let  $c_1^{-1}, c_2^{-1} \in \mathcal{W}_N$  and let  $\omega^2$  satisfy Assumption 2.8. Then, there exists a positive constant  $K$ , depending on  $A, r_1, L$ , such that,*

$$(2.24) \quad \|c_1^{-2} - c_2^{-2}\|_{L^2(\Omega)} \leq \frac{1}{\omega^2} e^{K(1+\omega^2 B_2)(|\Omega|/r_0^3)^{\frac{4}{7}}} \|\Lambda_{\omega^2 c_1^{-2}} - \Lambda_{\omega^2 c_2^{-2}}\|_{\mathcal{L}(H^{1/2}(\partial\Omega), H^{-1/2}(\partial\Omega))}.$$

*Proof.* To prove our stability estimate we follow the idea of Alessandrini of using CGO solutions but we use slightly different ones than those introduced in [20] and in [1] to obtain better constants in the stability estimates as proposed by [10]. We also use the estimates proposed in [10] (see Theorem 4.4) and due to [12] concerning the case of bounded potentials.

In fact, by Theorem 4.3 of [10], since  $c^{-2} \in L^\infty(\Omega)$ ,  $\|c^{-2}\|_{L^\infty(\Omega)} \leq B_2$ , there exists a positive constant  $C = C(\omega^2, B_2, A, r_1)$  such that for every  $\zeta \in \mathbb{C}^3$  satisfying  $\zeta \cdot \zeta = 0$  and  $|\zeta| \geq C$  the equation

$$-\Delta u - \omega^2 c^{-2} u = 0$$

has a solution of the form

$$u(x) = e^{ix \cdot \zeta} (1 + R(x))$$

where  $R \in H^1(\Omega)$  satisfies

$$\|R\|_{L^2(\Omega)} \leq \frac{C}{|\zeta|}, \quad \|\nabla R\|_{L^2(\Omega)} \leq C.$$

Let  $\xi \in \mathbb{R}^3$  and let  $\tilde{\omega}_1$  and  $\tilde{\omega}_2$  be unit vectors of  $\mathbb{R}^3$  such that  $\{\tilde{\omega}_1, \tilde{\omega}_2, \xi\}$  is an orthogonal set of vectors of  $\mathbb{R}^3$ . Let  $s$  be a positive parameter to be chosen later and set for  $k = 1, 2$ ,

$$(2.25) \quad \zeta_k = \begin{cases} (-1)^{k-1} \frac{s}{\sqrt{2}} (\sqrt{(1 - \frac{|\xi|^2}{2s^2})} \tilde{\omega}_1 + (-1)^{k-1} \frac{1}{\sqrt{2s}} \xi + i \tilde{\omega}_2) & \text{for } \frac{|\xi|}{\sqrt{2s}} < 1, \\ (-1)^{k-1} \frac{s}{\sqrt{2}} ((-1)^{k-1} \frac{1}{\sqrt{2s}} \xi + i (\sqrt{\frac{|\xi|^2}{2s^2} - 1}) \tilde{\omega}_1 + \tilde{\omega}_2)) & \text{for } \frac{|\xi|}{\sqrt{2s}} \geq 1. \end{cases}$$

Then an straightforward computation gives

$$\zeta_k \cdot \zeta_k = 0$$

for  $k = 1, 2$  and

$$\zeta_1 + \zeta_2 = \xi.$$

Furthermore, for  $k = 1, 2$ ,

$$(2.26) \quad |\zeta_k| = \begin{cases} s & \text{for } \frac{|\xi|}{\sqrt{2}s} < 1, \\ \frac{|\xi|}{\sqrt{2}} & \text{for } \frac{|\xi|}{\sqrt{2}s} \geq 1. \end{cases}$$

Hence,

$$(2.27) \quad |\zeta_k| = \max\{s, \frac{|\xi|}{\sqrt{2}}\}.$$

Then, by Theorem 4.3 of [10], for  $|\zeta_1|, |\zeta_2| \geq C_1 = \max\{C_0\omega^2 B_2, 1\}$ , with  $C_0 = C_0(A, r_1)$ , there exist  $u_1, u_2$ , solutions to  $-\Delta u_k - \omega^2 c_k^{-2} u_k = 0$  for  $k = 1, 2$  respectively, of the form

$$(2.28) \quad u_1(x) = e^{ix \cdot \zeta_1} (1 + R_1(x)), \quad u_2(x) = e^{ix \cdot \zeta_2} (1 + R_2(x))$$

with

$$(2.29) \quad \|R_k\|_{L^2(\Omega)} \leq \frac{C_0 \sqrt{|\Omega|}}{s} \omega^2 B_2$$

and

$$(2.30) \quad \|\nabla R_k\|_{L^2(\Omega)} \leq C_0 \sqrt{|\Omega|} \omega^2 B_2$$

for  $k = 1, 2$ . It is common in the literature to use estimates which contain  $\sqrt{|\Omega|}$ ; Different estimates in terms of  $|\Omega|$  are possible and just change the leading constant  $C_0$ .

Consider again Alessandrini's identity

$$\int_{\Omega} \omega^2 (c_1^{-2} - c_2^{-2}) u_1 u_2 dx = \langle (\Lambda_1 - \Lambda_2) u_1|_{\partial\Omega}, u_2|_{\partial\Omega} \rangle,$$

where  $u_k \in H^1(\Omega)$  is any solution of  $-\Delta u_k - \omega^2 c_k^{-2} u_k = 0$  and  $\Lambda_k = \Lambda_{\omega^2 c_k^{-2}}$  for  $k = 1, 2$ . Inserting the solutions (2.28) in Alessandrini's identity we derive

$$(2.31) \quad \begin{aligned} & \left| \int_{\Omega} \omega^2 (c_1^{-2} - c_2^{-2}) e^{i\xi \cdot x} dx \right| \\ & \leq \|\Lambda_1 - \Lambda_2\| \|u_1\|_{H^{1/2}(\partial\Omega)} \|u_2\|_{H^{1/2}(\partial\Omega)} + \left| \int_{\Omega} \omega^2 (c_1^{-2} - c_2^{-2}) e^{i\xi \cdot x} (R_1 + R_2 + R_1 R_2) dx \right| \\ & \leq \|\Lambda_1 - \Lambda_2\| \|u_1\|_{H^1(\Omega)} \|u_2\|_{H^1(\Omega)} + E(\|R_1\|_{L^2(\Omega)} + \|R_2\|_{L^2(\Omega)} + \|R_1\|_{L^4(\Omega)} \|R_2\|_{L^4(\Omega)}). \end{aligned}$$

where  $E := \|\omega^2 (c_1^{-2} - c_2^{-2})\|_{L^2(\Omega)}$ . By (2.29), (2.30), (2.27) and since  $\Omega \subset B_{2R}(0)$  we have

$$\|u_k\|_{H^1(\Omega)} \leq C \sqrt{|\Omega|} (s + |\xi|) e^{Ar_1(s+|\xi|)}, \quad k = 1, 2.$$

Let  $s \geq C_2$  so that  $s + |\xi| \leq e^{Ar_1(s+|\xi|)}$ . Then, for  $s \geq C_3 = \max(C_1, C_2)$ , using (2.29), (2.30) and the standard interpolation inequality ( $\|u\|_{L^4(\Omega)} \leq \|u\|_{L^6(\Omega)}^{3/4} \|u\|_{L^2(\Omega)}^{1/4}$ ) we get

$$(2.32) \quad |\omega^2 (c_1^{-2} - c_2^{-2}) \hat{(\xi)}| \leq C \sqrt{|\Omega|} \left( e^{4Ar_1(s+|\xi|)} \|\Lambda_1 - \Lambda_2\| + \frac{\omega^2 B_2 E}{s} \right)$$

where the  $\omega^2 c_k^{-2}$ 's have been extended to all  $\mathbb{R}^3$  by zero and  $\hat{\cdot}$  denotes the Fourier transform. Hence, from (2.32), we get

$$\int_{|\xi| \leq \rho} |\omega^2(c_1^{-2} - c_2^{-2})\hat{c}(\xi)|^2 d\xi \leq C|\Omega|\rho^3 \left( e^{8Ar_1(s+\rho)} \|\Lambda_1 - \Lambda_2\|^2 + \frac{\omega^4 B_2^2 E^2}{s^2} \right)$$

and hence

$$\begin{aligned} \|\omega^2(c_1^{-2} - c_2^{-2})\hat{c}\|_{L^2(\mathbb{R}^3)}^2 &\leq C|\Omega|\rho^3 \left( e^{8Ar_1(s+\rho)} \|\Lambda_1 - \Lambda_2\|^2 + \frac{\omega^4 B_2^2 E^2}{s^2} \right) \\ (2.33) \quad &+ \int_{|\xi| \geq \rho} |\omega^2(c_1^{-2} - c_2^{-2})\hat{c}(\xi)|^2 d\xi \end{aligned}$$

where  $C = C(A, r_1)$ . By (2.21) and (2.23) we have that

$$\|\omega^2(c_1^{-2} - c_2^{-2})\|_{H^{s'}(\Omega)}^2 \leq \frac{C}{r_0^{2s'}} E^2,$$

where  $C$  depends on  $L, s'$  and hence

$$\begin{aligned} \rho^{2s'} \int_{|\xi| \geq \rho} |\omega^2(c_1^{-2} - c_2^{-2})\hat{c}(\xi)|^2 d\xi &\leq \int_{|\xi| \geq \rho} |\xi|^{2s'} |\omega^2(c_1^{-2} - c_2^{-2})\hat{c}(\xi)|^2 d\xi \\ &\leq \int_{\mathbb{R}^3} (1 + |\xi|^2)^{s'} |\omega^2(c_1^{-2} - c_2^{-2})\hat{c}(\xi)|^2 d\xi \leq \frac{C}{r_0^{2s'}} E^2. \end{aligned}$$

Hence, we get

$$\int_{|\xi| \geq \rho} |\omega^2(c_1^{-2} - c_2^{-2})\hat{c}(\xi)|^2 d\xi \leq \frac{CE^2}{r_0^{2s'} \rho^{2s'}}$$

for every  $s' \in (0, 1/2)$ . Inserting last bound in (2.33) we derive

$$\|\omega^2(c_1^{-2} - c_2^{-2})\hat{c}\|_{L^2(\mathbb{R}^3)}^2 \leq C \left( \rho^3 |\Omega| e^{8Ar_1(s+\rho)} \|\Lambda_1 - \Lambda_2\|^2 + \rho^3 |\Omega| \frac{\omega^4 B_2^2 E^2}{s^2} + \frac{E^2}{r_0^{2s'} \rho^{2s'}} \right).$$

where  $C = C(L, s')$ . To make the last two terms in the right-hand side of the inequality of equal size we pick up

$$\sqrt[3]{|\Omega|} \rho = \left( \frac{|\Omega|}{r_0^3} \right)^{\frac{2s'}{3(3+2s')}} \left( \frac{1}{\alpha} \right)^{\frac{1}{3+2s'}} s^{\frac{2}{3+2s'}}$$

with  $\alpha = \max\{1, \omega^4 B_2^2\}$ . Then, by Assumption 2.6 and observing that we might assume without loss of generality that  $\frac{|\Omega|}{r_0^3} > 1$ . In fact, if this is not the case we can choose a smaller value of  $r_0$  so that the condition is satisfied.

$$\|\omega^2(c_1^{-2} - c_2^{-2})\|_{L^2(\Omega)}^2 \leq CE^2 \left( \frac{|\Omega|}{r_0^3} \right)^{\frac{2s'}{3+2s'}} \left( e^{C_4 \left( \frac{|\Omega|}{r_0^3} \right)^{\frac{2s'}{3(3+2s')}} s} \left( \frac{\|\Lambda_1 - \Lambda_2\|}{E} \right)^2 + \left( \frac{\alpha}{s^2} \right)^{\frac{2s'}{3+2s'}} \right)$$

for  $s \geq C_3$  and where  $C$  depends on  $s', L, A, r_1$  and  $C_4$  depends on  $L, A, r_1$ . We now make the substitution

$$s = \frac{1}{C_4 \left( \frac{|\Omega|}{r_0^3} \right)^{\frac{2s'}{3(3+2s')}}} \left| \log \frac{\|\Lambda_1 - \Lambda_2\|}{E} \right|$$

where we assume that

$$\frac{\|\Lambda_1 - \Lambda_2\|}{E} < c := e^{-\bar{C} \max\{1, \omega^2 B_2\} \left(\frac{|\Omega|}{r_0^3}\right)^{\frac{2s'}{3(3+2s')}}}$$

with  $\bar{C} = \bar{C}(R)$  in order that the constraint  $s \geq C_3$  is satisfied. Under this assumption,

$$(2.34) \quad \|\omega^2(c_1^{-2} - c_2^{-2})\|_{L^2(\Omega)} \leq C(\sqrt{\alpha})^{\frac{2s'}{3+2s'}} \left(\frac{|\Omega|}{r_0^3}\right)^{\frac{2s'}{3+2s'} \frac{9+10s'}{6(3+2s')}} E \left( \left| \log \frac{\|\Lambda_1 - \Lambda_2\|}{E} \right|^{-\frac{2s'}{3+2s'}} \right)$$

where  $C = C(L, s', A, r_1)$  and we can rewrite last inequality in the form

$$(2.35) \quad E \leq C(1 + \omega^2 B_2)^{\frac{2s'}{3+2s'}} \left(\frac{|\Omega|}{r_0^3}\right)^{\frac{2s'}{3+2s'} \frac{9+10s'}{6(3+2s')}} E \left( \left| \log \frac{\|\Lambda_1 - \Lambda_2\|}{E} \right|^{-\frac{2s'}{3+2s'}} \right)$$

which gives

$$(2.36) \quad E \leq e^{C(1+\omega^2 B_2) \left(\frac{|\Omega|}{r_0^3}\right)^{\frac{9+10s'}{6(3+2s')}}} \|\Lambda_1 - \Lambda_2\|$$

where  $C = C(L, s', A, r_1)$ . On the other hand if

$$\frac{\|\Lambda_1 - \Lambda_2\|}{E} \geq c,$$

then

$$(2.37) \quad \|\omega^2(c_1^{-2} - c_2^{-2})\|_{L^2(\Omega)} \leq c^{-1} \|\Lambda_1 - \Lambda_2\| \leq e^{\bar{C}(1+\omega^2 B_2) \left(\frac{|\Omega|}{r_0^3}\right)^{\frac{1}{3(3+2s')}}} \|\Lambda_1 - \Lambda_2\|$$

Hence, from (2.36) and (2.37) and recalling that  $s' \in (0, \frac{1}{2})$ , we have that

$$(2.38) \quad E \leq e^{C(1+\omega^2 B_2) \left(\frac{|\Omega|}{r_0^3}\right)^{\frac{9+10s'}{6(3+2s')}}} \|\Lambda_1 - \Lambda_2\|$$

Choosing  $s' = \frac{1}{4}$ , we derive

$$\|c_1^{-2} - c_2^{-2}\|_{L^2(\Omega)} \leq \frac{1}{\omega^2} e^{K(1+\omega^2 B_2) \left(|\Omega|/r_0^3\right)^{\frac{4}{7}}} \|\Lambda_1 - \Lambda_2\|$$

where  $K = K(L, A, r_1, s')$  and the claim follows.  $\square$

REMARK 2.11. Here we state an  $L^\infty$ -stability estimate, in contrast to the  $L^2$ -stability estimate in Proposition 2.10.

Observing that

$$\frac{1}{\sqrt{|\Omega|}} \|c_1^{-2} - c_2^{-2}\|_{L^2(\Omega)} \leq \|c_1^{-2} - c_2^{-2}\|_{L^\infty(\Omega)} \leq \frac{C}{r_0^{3/2}} \|c_1^{-2} - c_2^{-2}\|_{L^2(\Omega)},$$

where  $C = C(L)$ , and we immediately get the following stability estimate in the  $L^\infty$  norm

$$\|c_1^{-2} - c_2^{-2}\|_{L^\infty(\Omega)} \leq \frac{C}{\omega^2} e^{K(1+\omega^2 B_2) \left(|\Omega|/r_0^3\right)^{\frac{4}{7}}} \|\Lambda_1 - \Lambda_2\|$$

with  $C = C(L)$ .

REMARK 2.12. In [6] the following lower bound of the stability constant has been obtained in the case of a uniform polyhedral partition  $\mathcal{D}_N$

$$(2.39) \quad C_N \geq \frac{1}{4\omega^2} e^{K_1 N^{\frac{1}{5}}}$$

Choose a uniform cubical partition  $\mathcal{D}_N$  of  $\Omega$  of mesh size  $r_0$ . Then,

$$|\Omega| = N r_0^3$$

and estimate (2.24) of Proposition 2.10 gives

$$(2.40) \quad C_N = \frac{1}{\omega^2} e^{K(1+\omega^2 B_2)N^{\frac{4}{7}}},$$

which proves a sharp bound on the Lipschitz constant with respect to  $N$  when the global DtN map is known. In [6] a Lipschitz stability estimate has been derived in terms of the local DtN map using singular solutions. This type of solutions allows to recover the unknown piecewise constant wavespeeds by determining it on the outer boundary of the domain and then, by propagating the singularity inside the domain, to recover step by step the wavespeed on the interface of all subdomains of the partition. This iterative procedure does not lead to sharp bounds of the Lipschitz constant appearing in the stability estimate. It would be interesting if one can get a better bound of the Lipschitz constant using oscillating solutions.

REMARK 2.13. In Lemma 2.5 we have seen that  $F_\omega$  is Fréchet differentiable with Lipschitz derivative  $DF_\omega$  for which we have derived an upper bound in terms of the a priori data. From the stability estimates we can easily derive the following lower bound

$$(2.41) \quad \min_{c^{-2} \in \mathcal{W}_N; \delta c \in \mathbb{R}^N, \|\delta c\|_{L^\infty(\Omega)}=1} \|DF_\omega[c^{-2}]\delta c\|_* \geq \omega^2 e^{-K(1+\omega^2 B_2)(\frac{|\Omega|}{r_0^3})^{4/7}}.$$

where  $K = K(L, A, r_1)$  and  $\|\cdot\|_*$  indicates the norm in  $\mathcal{L}(H^{1/2}(\partial\Omega), H^{-1/2}(\partial\Omega))$  i.e.

$$\|T\|_* = \sup\{\langle Tg, h \rangle : g, h \in H^{1/2}(\partial\Omega), \|g\|_{H^{1/2}(\partial\Omega)} = \|h\|_{H^{1/2}(\partial\Omega)} = 1\}$$

In fact, by the injectivity of  $DF_\omega$

$$\min_{c^{-2} \in \mathcal{W}_N; \delta c \in \mathbb{R}^N, \|\delta c\|_{L^\infty(\Omega)}=1} \|DF_\omega[c^{-2}]\delta c\|_* = m_0/2 > 0$$

Then, there exists  $\delta c_0$  satisfying  $\|\delta c_0\|_{L^\infty(\Omega)} = 1$  and  $c_0^{-2} \in \mathcal{W}_N$  such that

$$\|DF_\omega[c_0^{-2}]\delta c_0\|_* \leq m_0.$$

Hence, by the definition of  $\|\cdot\|_*$  it follows that

$$|\langle DF_\omega[c_0^{-2}](\delta c_0)g, h \rangle| = \left| \int_\Omega \delta c \tilde{u}_0 v_0 \right| \leq m_0 \|\tilde{u}_0\|_{H^{1/2}(\partial\Omega)} \|v_0\|_{H^{1/2}(\partial\Omega)}$$

where  $\tilde{u}_0$  and  $v_0$  are solutions to the equation  $(-\Delta - \omega^2 c_0^{-2})u = 0$  in  $\Omega$  with boundary data  $g$  and  $h$  respectively. Proceeding like in the proof of the stability result (Proposition 2.10) and Remark 2.11 we derive that

$$1 = \|\delta c_0^{-2}\|_{L^\infty(\Omega)} \leq \frac{1}{\omega^2} e^{K(1+\omega^2 B_2)(\frac{|\Omega|}{r_0^3})^{4/7}} m_0$$

which gives the lower bound (2.41).

**3. Computational experiments.** In this section, we numerically compute quantitative stability estimates for the inverse problem associated with the Dirichlet-to-Neumann map. We illustrate the stability behaviour and compare with the analytical bounds formulated in Section 2. In particular we consider the seismic reconstruction problem for which the data are usually partial and only located at the surface, with the objective of recovering subsurface structures. In this context the two models  $c_1$  and  $c_2$  in the stability formulation can be assimilated to the target subsurface medium and the ‘initial’ guess. The stability constant is of fundamental importance for the reconstruction algorithm to guarantee the convergence; In particular we mention the full waveform inversion method, where the recovery follows an iterative minimization of the difference between the data and simulations using the initial guess (see [22, 19]).

We develop two methods to estimate the stability, the first one is based on the direct definition of the constant, and requires the knowledge of both models,  $c_1$  and  $c_2$ . A more realistic approach for seismic inverse problem is to assume that one of the subsurface models is unknown (the target model, say  $c_1$ ) while the other (say  $c_2$ ) would be the known initial guess or current iterate. Here only one of the two models is explicitly known. Hence this second estimation is based on the lower bound of the Fréchet derivative following the linearization of the problem as developed in Remark 2.13. This second numerical estimate involves the Gauss-Newton Hessian and only requires the knowledge of  $c_2$ .

The model (wavespeed) is defined on a cubical (structured) domain partition of a rectangular block. With increasing  $N$ , the size of the cubes decreases, possibly non uniformly. We use piecewise constant functions on the cubes to define the wavespeeds following the main assumption for the Lipschitz stability to hold. Such a partition can be related to Haar wavelets, where  $N$  determines the scale. These naturally introduce approximate representations, that is, when the scale of the approximation is coarser than the finest scale contained in the model.

The numerical discretization of the operator is realized using compact finite differences, where Dirichlet boundary conditions are invoked, the top boundary is considered as a free surface. The Dirichlet sources at the top boundary introduce Identity block in the discretized Helmholtz operator and give the following linear problem

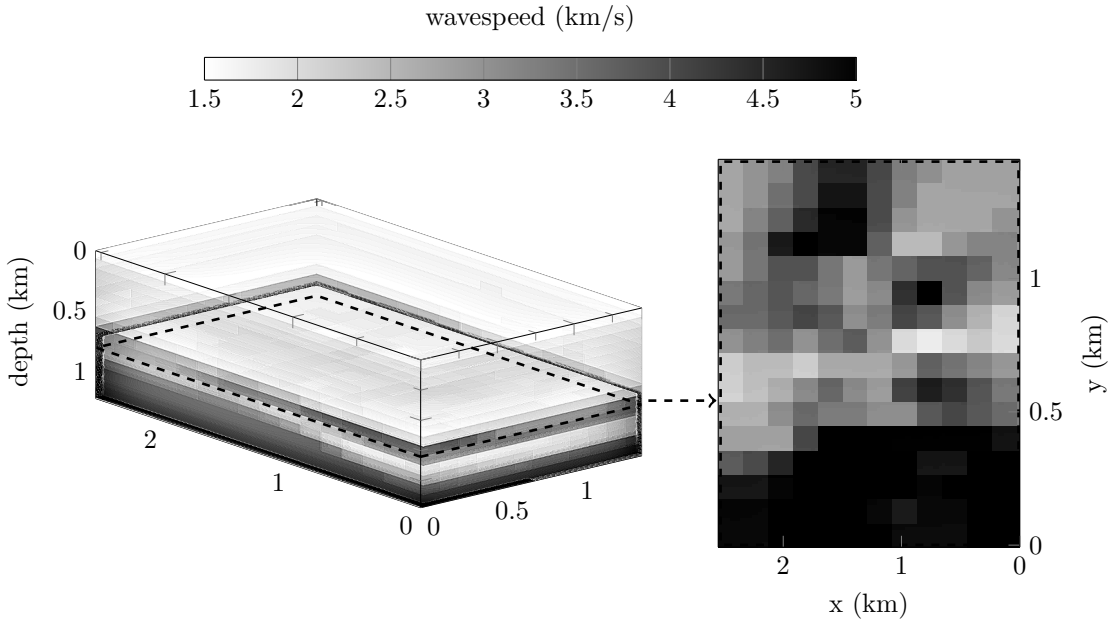
$$(3.1) \quad \begin{pmatrix} A_{ii} & A_{i\partial} \\ A_{\partial i} & A_{\partial\partial} \end{pmatrix} \begin{pmatrix} u_i \\ u_\partial \end{pmatrix} = \begin{pmatrix} A_{ii} & A_{i\partial} \\ 0 & Id \end{pmatrix} \begin{pmatrix} u_i \\ u_\partial \end{pmatrix} = \begin{pmatrix} 0 \\ g \end{pmatrix},$$

where  $A$  represents the discretized operator,  $i$  labels interior points and  $\partial$  labels boundary points,  $g$  has values at the source location and is zero elsewhere (free surface). This system verifies  $u_\partial = u|_{\partial\Omega} = g$  (i.e. Dirichlet boundary condition) and  $A_{ii}u_i + A_{i\partial}u|_{\partial\Omega} = 0$ .

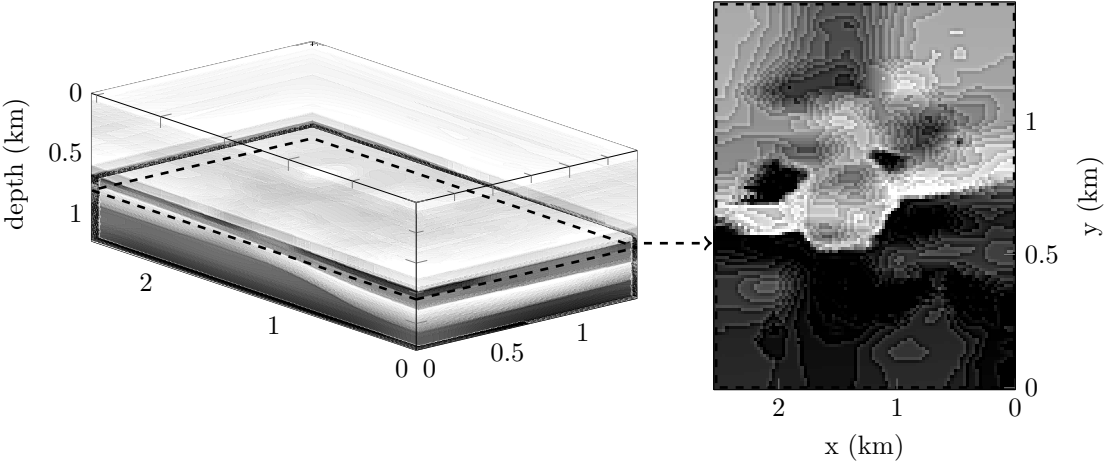
A massively parallel direct structured solver is employed for the solution of the linear system, following the work of [23, 24]. The Neumann data are generated by taking the normal derivative of the solution wavefield  $u$ , at the receiver locations.

Our experiments use a three dimensional model of size  $2.55 \times 1.45 \times 1.22$  km. The wavespeed  $c_1$  is viewed as a reference model (which is known in this test case) and is represented Figure 1 (courtesy Statoil). We also illustrate the different partitions of a model and the notion of approximation. Obviously the larger the number of subdomains is, the more precise will the representation be.

In our experiments, Gaussian shaped (spatial) source functions (see Figure 2(c)) are applied at the top boundary following the Dirichlet-to-Neumann map. We define a set of sources separated by 160m along the  $x$ -axis and 150m along  $y$ -axis to generate a regular map of  $16 \times 10$  points, where the boundaries are avoided. The receivers are positioned in the same fashion every 60m along the  $x$ -axis and 45m along  $y$ -axis and generate a regular map of  $43 \times 32$  points, see Figures 2(a) and 2(b). Hence we consider the geophysical settings with partial boundary data, obtained from several sources. We illustrate the data obtained from a single centered boundary shot at 5Hz frequency Figure 2(d).



(a) Partition using  $N = 2,880$  domains.



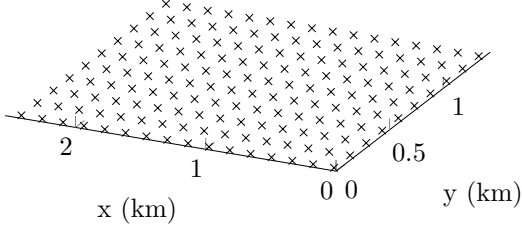
(b) Partition using  $N = 1,527,168$  domains.

FIG. 1. Three dimensional representations and horizontal sections at 800m depth of the reference wavespeed ( $c_1$ ) using different partition, i.e. scales. Every scale has a structured (rectangular) decomposition using piecewise constant. The size of the rectangular boxes defines the scale of the wavespeed.

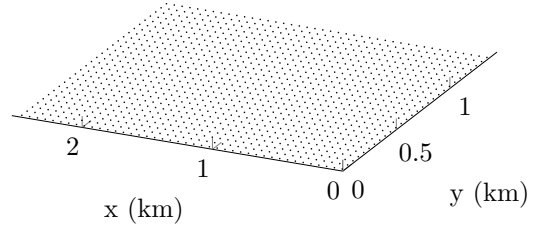
For the computation of the stability estimates we consider  $c_2$  as the model shown in Figure 3. This setup can be associated with the ‘true’ subsurface Figure 1 and starting model Figure 3. In this context we have chosen the initial guess with no knowledge of any structures by simply considering a one dimensional variation in depth.

**3.1. Direct computational stability estimates.** We estimate the stability constant from its definition,

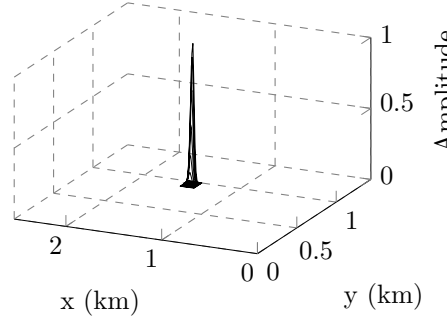
$$(3.2) \quad \|c_1^{-2} - c_2^{-2}\|^2 < \mathcal{C} \|F_\omega(c_1^{-2}) - F_\omega(c_2^{-2})\|^2,$$



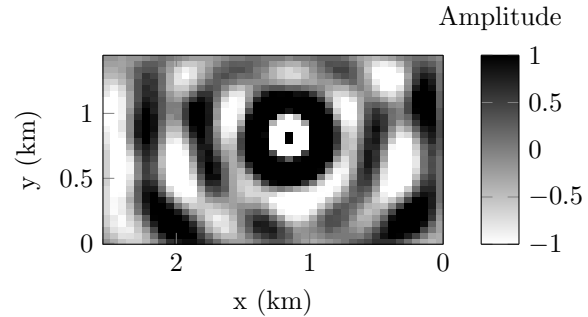
(a) the crosses represent the boundary sources locations.



(b) The lattice represents the discretization of the data, i.e. the receivers location.



(c) Illustration of the source shape for a localized boundary source.



(d) Data recovered from a boundary centered shot, i.e. wavefield measured at the receivers location.

FIG. 2. Illustration of the acquisition set and generated data.

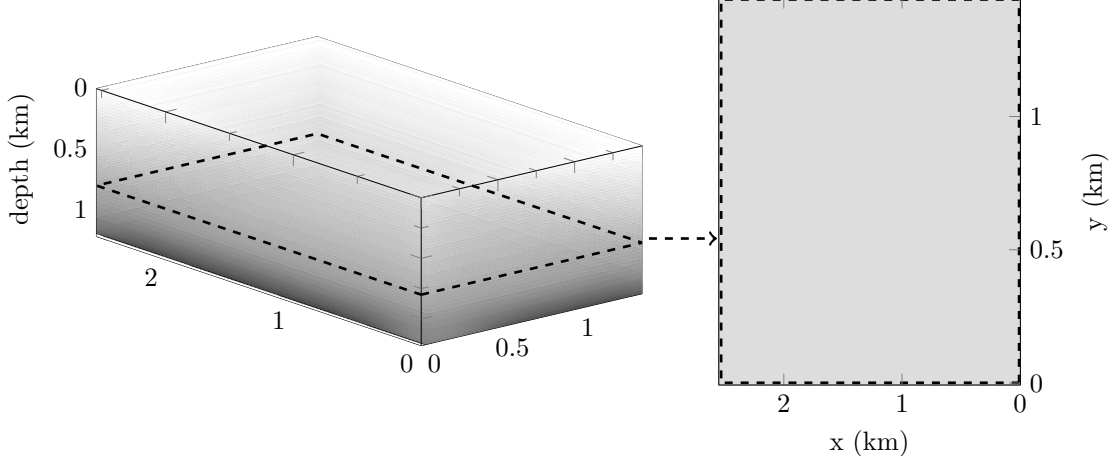


FIG. 3. Three dimensional wavespeed used for the successive estimation of the stability constant ( $c_2$ ), 3D representation (left) and horizontal sections at 800m depth (right).

where  $c_1$  has been given Figure 1 and  $c_2$  Figure 3. Here  $\|c_1^{-2} - c_2^{-2}\|$  denotes the  $L^2$ -norm of the functions from the finite dimensional Ansatz space. We note that this expression does not depend on the frequency but only on the partition selected. On the right is the difference between the observed data ( $F_\omega(c_2^{-2})$ ) and the measurements ( $F_\omega(c_1^{-2})$ ), according to the acquisition set (sources and receivers location). In our experiments we have generated synthetic data using a different method for the discretization of the operator and a different solver, in order to avoid inverse crime. Hence at a

selected partition (number of domains) and frequency, we simulate data and compute the difference with the measurements, from which we deduce the stability constant following Equation (3.2).

The numerical estimates for the stability constant  $\mathcal{C}$  should depend on the number of domains  $N$  following the expression of the lower and upper bounds defined in the Remark 2.12, Equations (2.39) and (2.40). Thus we fix the frequency and estimate the stability for different partitions. The evolution of the estimates and underlying bounds are presented in Figure 4 at two selected frequencies, 5 and 10Hz. We plot on a log log scale the function  $\log(\mathcal{C}\omega^2)$  to focus on the power of  $N$  in the estimates, which is the slope of the lines (4/7 for the upper bound and 1/5 for the lower bound).

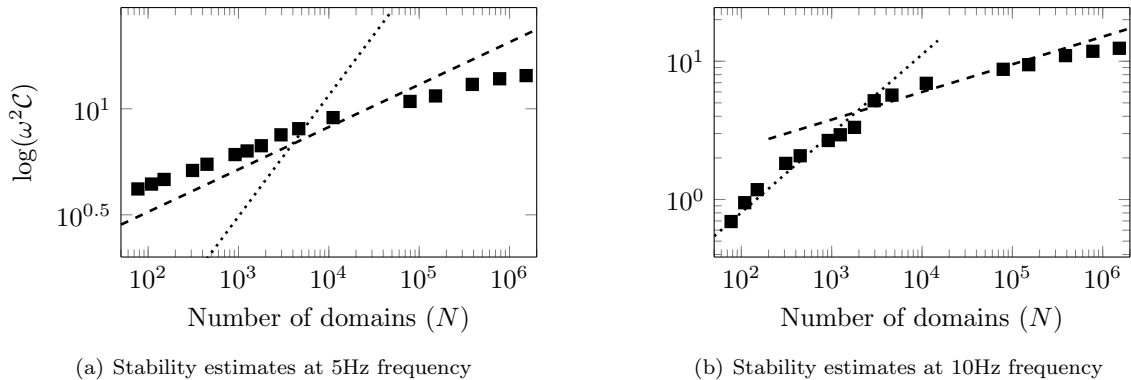


FIG. 4. The black squares represent the computational estimates of the stability constant (■) depending on the number of domains  $N$  at selected frequency. The dashed line (—) represents the analytical lower bound and the dotted line (..) the upper bound, estimated with Equation (3.3).

Regarding the different coefficients in the analytical bounds,  $K$  and  $K_1$  remain undecided and are numerically approximated so that the bounds match the estimates at best. For instance the numerical value for  $K_1$  is obtained from Equation (2.39) by computing the average value based on the numerical stability estimates and  $K$  is approximated following the same principle:

$$(3.3) \quad K_1 = \frac{1}{n_{st}} \sum_{i=1}^{n_{st}} \frac{\log(4\omega^2 \mathcal{C}_i)}{N_i^{1/5}}, \quad K = \frac{1}{n_{st}} \sum_{i=1}^{n_{st}} \frac{\log(\omega^2 \mathcal{C}_i)}{(1 + \omega^2 B_2) N_i^{4/7}}.$$

Here,  $n_{st}$  is the number of numerical stability constant estimates and  $\mathcal{C}_i$  the corresponding estimate for partitioning  $N_i$ . The numerical values obtained are given Table 3.1. We also note that the term  $\omega^2 B_2$  of the upper bound Equation (2.40) is relatively small in the geophysical context as we have here  $B_2 = 5.10^{-7}$ .

We can see that the stability constant increases with the number of subdomains, as expected. There are clearly two states in the evolution of the estimates at the highest frequency (10Hz, Figure 4(b)). For a low number of partitions  $N$  the numerical estimates match particularly well the upper bound while at finer scale it follows accurately the lower bound. This is illustrated in Figure 5 where we decompose the two parts of the estimates between the low and high number of domains.

Alternatively for a lower frequency, i.e. 5Hz on Figure 4(a), the upper bound appears to blow up while the lower bound matches accurately the evolution of the stability constant estimates. Hence the upper bound we have obtained here is particularly appropriate for coarse scale and high frequency: when the variation of model is much coarser compared to the wavelength.

**3.2. Computational stability estimates via the Fréchet derivative.** In practical cases, the knowledge of the reference ('true') wavespeed is not realistic, and its reconstruction is actually

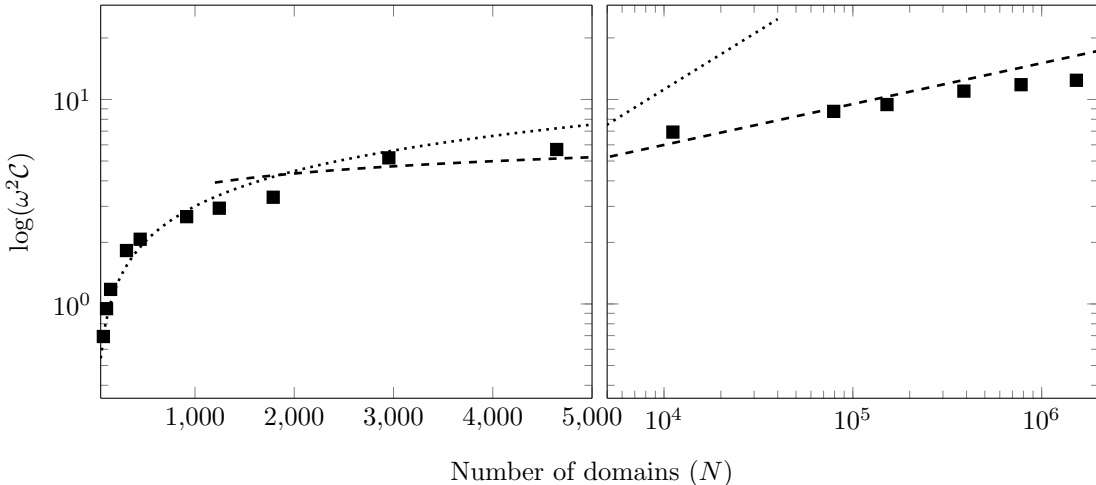


FIG. 5. The black squares represent the computational estimates of the stability constant ( $\blacksquare$ ) depending on the number of domains  $N$  at 10Hz. The left part shows the coarsest scales which match accurately the upper bound (dotted line,  $\dots$ ). On the right the finer scale estimates are accurately anticipated by the lower bound (dashed line,  $\dashdot$ ). The constants  $K$  and  $K_1$  for the computation of the lower and upper bounds are numerically approximated with values given Table 3.1, following Equation (3.3).

	5Hz	10Hz
$K_1$	1.3	1
$K$	0.06	0.06

TABLE 3.1

Numerical estimation of the constant in the analytical bounds formulation for the numerical estimates of the stability (Figure 4, with  $B_2 = (1/1400)^2$ ).

the goal of the inversion scheme. In such cases, it is not possible to estimate the stability constant using the direct method. Instead we have shown that the stability constant is linked with the lower bound of the Fréchet derivative in the Remark 2.13. Hence we estimate the stability constant with the Gauss-Newton Hessian, which is directly defined with the Fréchet derivative:  $H^{GN} = DF^*DF$ . Then the lower bound of the Fréchet derivative is computed as the square root of the lowest singular value of the Gauss-Newton Hessian. We use projections onto the different domain partitions, according to the scale. We note that the numerical computation of the Gauss-Newton Hessian (see, for example, [19]) does neither depend on the observed data, nor on the ‘true’ model. However, it does depend on the current (starting) model.

We compare the estimates obtained with the direct method and the Fréchet derivative (via the Gauss-Newton Hessian), in the case of the starting wavespeed  $c_2$  pictured on Figure 3. The numerical cost is obviously higher than the direct method, hence we limit ourselves to the first set of partitions. We compare both evolutions in Figure 6, where the estimates have been normalized.

Clearly the Gauss-Newton Hessian provides an accurate estimate of the stability constant without needing the knowledge of the model  $c_1$ . The general variation in the stability constant is identical, at the exception of the very coarse scale with a few domains.

The numerical estimation of the stability constant provides an useful indication of the stability behavior in a geophysical context. In particular the use of partial data, only located on the top surface, does not contradict the behavior given by the analytical bound. The dependency with the

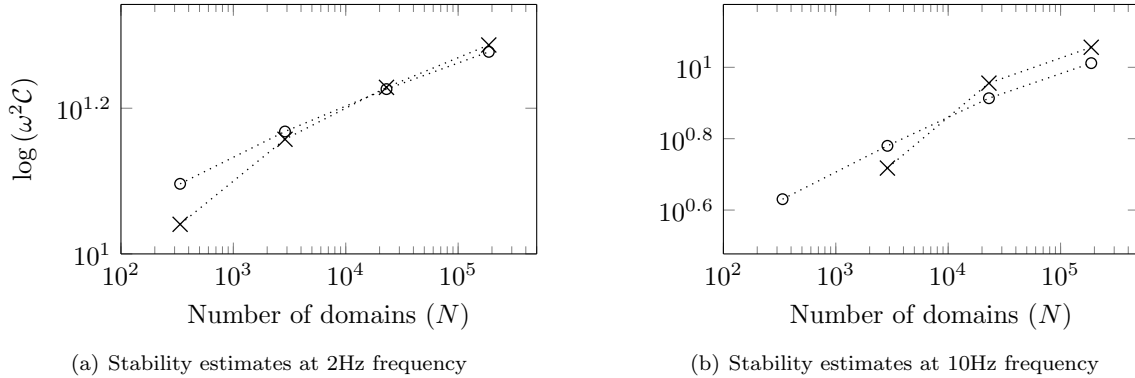


FIG. 6. The circles represents the computational estimates of the stability constants using the direct method ( $\cdot\circ\cdot$ ), the lower bound of the Fréchet derivative estimated via the Gauss-Newton Hessian singular value is represented with the crosses ( $\cdot\times\cdot$ ).

number of domains, at fixed frequency, is accurately anticipated. When the number of partitions is relatively small and the frequency relatively high, the stability behaves following the upper bound; on the contrary for lower frequencies, the stability behaves more likely following the lower bound. This can in particular be employed to guarantee the convergence of numerical algorithm for the reconstruction of subsurface materials.

**Acknowledgement.** This research was supported in part by the members, BGP, ExxonMobil, PGS, Statoil and Total, of the Geo-Mathematical Imaging Group now at Rice University. The work of OS is supported by the Austrian Science Fund (FWF), Project P26687-N25 Interdisciplinary Coupled Physics Imaging.

## REFERENCES

- [1] G. ALESSANDRINI, *Stable determination of conductivity by boundary measurements*, Appl. Anal., 27 (1988), pp. 153–172.
- [2] G. ALESSANDRINI AND S. VESSELLA, *Lipschitz stability for the inverse conductivity problem*, Adv. in Appl. Math., 35 (2005), pp. 207–241.
- [3] G. BAO AND P. LI, *Inverse medium scattering problems for electromagnetic waves*, SIAM J. Appl. Math., 65 (2005), pp. 2049–2066 (electronic).
- [4] G. BAO AND F. TRIKI, *Error estimates for the recursive linearization of inverse medium problems*, J. Comput. Math., 28 (2010), pp. 725–744.
- [5] H. BEN-HADJ-ALI, S. OPERTO, AND J. VIRIEUX, *Velocity model-building by 3d frequency-domain, full-waveform inversion of wide-aperture seismic data*, Geophysics, 73 (2008).
- [6] E. BERETTA, M. V. DE HOOP, AND L. QIU, *Lipschitz stability of an inverse boundary value problem for a Schrödinger-type equation*, SIAM J. Math. Anal., 45 (2013), pp. 679–699.
- [7] E. BERETTA AND E. FRANCINI, *Lipschitz stability for the electrical impedance tomography problem: the complex case*, Comm. Partial Differential Equations, 36 (2011), pp. 1723–1749.
- [8] K. D. BLAZEK, C. STOLK, AND W. W. SYMES, *A mathematical framework for inverse wave problems in heterogeneous media*, Inverse Problems, 29 (2013), p. 065001.
- [9] K. DATCHEV AND M. V. DE HOOP, *Iterative reconstruction of the wavespeed for the wave equation with bounded frequency boundary data*, arXiv preprint arXiv:1506.09014, (2015).
- [10] J. FELDMAN, M. SALO, AND G. UHLMANN, *The Calderón problem — An Introduction to Inverse Problems*, unpublished ed., 2015.
- [11] D. GILBARG AND N. S. TRUDINGER, *Elliptic partial differential equations of second order*, vol. 224 of Grundlehren der Mathematischen Wissenschaften [Fundamental Principles of Mathematical Sciences], Springer-Verlag, Berlin, second ed., 1983.
- [12] P. HÄHNER, *A periodic Faddeev-type solution operator*, J. Differential Equations, 128 (1996), pp. 300–308.
- [13] P. HÄHNER AND T. HOHAGE, *New stability estimates for the inverse acoustic inhomogeneous medium problem and applications*, SIAM Journal on Mathematical Analysis, 33 (2001), pp. 670–685.
- [14] T. HOHAGE, *Logarithmic convergence rates of the iteratively regularized gauss - newton method for an inverse potential and an inverse scattering problem*, Inverse Problems, 13 (1997), p. 1279.

- [15] R. MAGNANINI AND G. PAPI, *An inverse problem for the Helmholtz equation*, Inverse Problems, 1 (1985), pp. 357–370.
- [16] N. MANDACHE, *Exponential instability in an inverse problem for the Schrödinger equation*, Inverse Problems, 17 (2001), pp. 1435–1444.
- [17] S. NAGAYASU, G. UHLMANN, AND J.-N. WANG, *Increasing stability in an inverse problem for the acoustic equation*, Inverse Problems, 29 (2013), p. 025012.
- [18] R. G. NOVIKOV, *New global stability estimates for the Gel'fand-Calderon inverse problem*, Inverse Problems, 27 (2011), p. 015001.
- [19] R. G. PRATT, C. SHIN, AND G. J. HICKS, *Gauss-newton and full newton methods in frequency-space seismic waveform inversion*, Geophysical Journal International, 133 (1998), pp. 341–362.
- [20] J. SYLVESTER AND G. UHLMANN, *A global uniqueness theorem for an inverse boundary value problem*, Ann. of Math. (2), 125 (1987), pp. 153–169.
- [21] W. W. SYMES, *The seismic reflection inverse problem*, Inverse Problems, 25 (2009), pp. 123008, 39.
- [22] A. TARANTOLA, *Inversion of seismic reflection data in the acoustic approximation*, Geophysics, 49 (1984), pp. 1259–1266.
- [23] S. WANG, M. V. DE HOOP, AND J. XIA, *On 3d modeling of seismic wave propagation via a structured parallel multifrontal direct helmholtz solver*, Geophysical Prospecting, 59 (2011), pp. 857–873.
- [24] S. WANG, M. V. DE HOOP, J. XIA, AND X. S. LI, *Massively parallel structured multifrontal solver for time-harmonic elastic waves in 3-d anisotropic media*, Geophysical Journal International, 191 (2012), pp. 346–366.